Monte Carlo simulations of harmonic and anharmonic oscillators in discrete Euclidean time

DESY Summer Student Programme, 2014

Ronnie Rodgers
University of Oxford, United Kingdom

Laura Raes
University of Antwerp, Belgium

Supervisors
Karl Jansen
Krzysztof Cichy

5th of September 2014

Abstract

We study quantum harmonic and anharmonic oscillators in the path integral formulation, using the Metropolis Monte Carlo method to generate paths to calculate the lowest two energy levels and the ground state probability density. In addition, for the harmonic oscillator we make measurements of the autocorrelation time and other parameters in order to optimize our code.

Contents

1 Introduction

In this report we will make calculations of observables for both harmonic and anharmonic oscillators. We use the path integral formulation on a discrete Euclidean time lattice. The transformation to Euclidean time is made to allow us to perform Monte Carlo simulations to generate paths, which can be used to make measurements. For example, by measuring the position of the particle at each point on the time lattice, the mean square position can be determined.

1.1 Path integrals

In the path integral formulation of quantum mechanics, the amplitude (or kernel) for a particle to go from (x_a, t_a) to (x_b, t_b) is given by [1]

$$K(b,a) = \int_a^b \mathrm{e}^{iS/\hbar} \mathcal{D}x(t) \tag{1.1}$$

where S is the action for a path, and $\mathcal{D}x(t)$ means that the integration takes place over all possible paths. This means that rather than considering the particle as only travelling along one trajectory as in classical mechanics, all possible paths must be considered, and summed over with a phase factor $\mathrm{e}^{iS/\hbar}$. To define a path, we split the time interval $[t_a, t_b]$ into N segments of length ϵ. The path is then defined by the position of the particle at the start of each segment. In between these times, the particle can be assumed to be travelling in a straight line. For an example calculation of the kernel for a harmonic oscillator, see appendix A.

To make the connection to statistical mechanics, we perform a Wick rotation to Euclidean time. This means that we make the transformation $t \to it$. In 4 space-time dimenions this transformation leads to the metric diag(1, 1, 1, 1). We choose to use a forward difference method to discretize the derivative, giving the action as

$$S = \epsilon \sum_{i=0}^{N} \left(\frac{m(x_{i+1} - x_i)^2}{2\epsilon^2} + V(x_i) \right) \tag{1.2}$$

and so the kernel becomes

$$K(b,a) = \lim_{\epsilon \to 0} A(\epsilon) \int \cdots \int \exp\left[-\frac{1}{\hbar} \int_b^a \epsilon \sum_{i=0}^{N-1} \left(\frac{m(x_{i+1} - x_i)^2}{2\epsilon^2} + V(x_i) \right) dt \right] dx_1 \cdots dx_{N-1} \tag{1.3}$$

This can be recognised as the partition function for a lattice of $N-1$ sites, with the imaginary time Lagrangian in place of the Hamiltonian, and $\hbar$ replacing $k_B T$.

1.2 Oscillators

In this report we study both harmonic and anharmonic oscillators, with action (again using a forward difference derivative) given by:

$$S = a \sum_{i=0}^{N} \left(\frac{m(x_{i+1} - x_i)^2}{2a^2} + \frac{1}{2}\mu^2 x_i^2 + \lambda x_i^4 \right) \tag{1.4}$$

with $\mu^2 > 0$, $\lambda = 0$ for the harmonic oscillator, and μ^2 arbitrary, $\lambda > 0$ for the anharmonic oscillator. Periodic boundary conditions $x_{N+1} = x_0$ have been used, and the time lattice spacing is now written as a. N and a must be picked such that $T = Na$ is larger than the timescale of the oscillator, given by $T_E = 2\pi\hbar/E_0$, where E_0 is the ground state energy [2]. Throughout this report, we fix $T = 100$, which is sufficient for all of the sets of parameters we use. In general, it is important the check that T is larger than T_E.

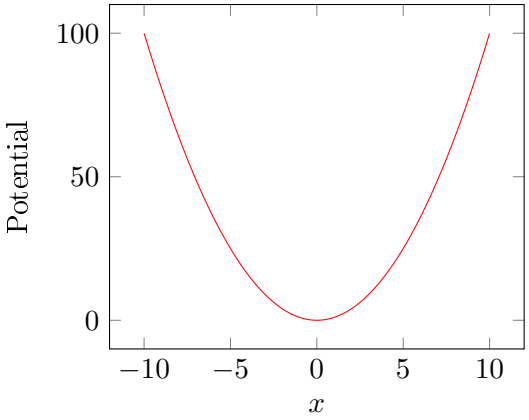

Figure 1.1: Harmonic oscillator potential with $\mu^2 = 1$, $m = 1$.

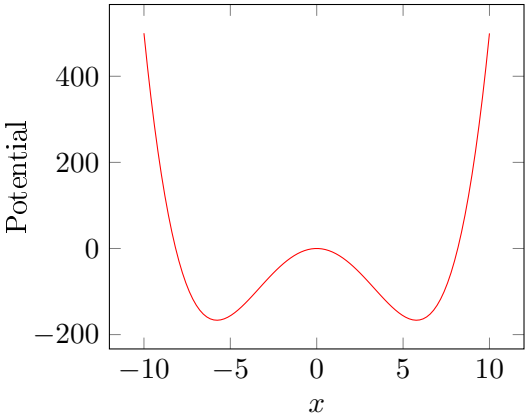

Figure 1.2: Anharmonic oscillator potential with $\mu^2 = -10$, $\lambda = 0.15$, $m = 1$.

1.3 Measuring observables

In our imaginary time formalism, paths are distributed according to the Boltzmann probability distribution [2]:

$$P[x(t)]\mathcal{D}x(t) = \frac{\exp(-S/\hbar)\mathcal{D}x(t)}{\int \exp(-S/\hbar)\mathcal{D}x(t)} \tag{1.5}$$

We use the Metropolis algorithm to randomly generate paths, which must follow the same distribution. When the paths are being generated according to this distribution, we say they are in (thermal) equilibrium. By taking measurements over many such paths, the values of observables may then be calculated. In such a way, we calculate the mean square position $\langle x^2 \rangle$, the ground state probability distribution, and the energies of the lowest two energy levels.

2 Generating an equilibrium state

2.1 The Metropolis algorithm

In order to generate our quantum mechanical paths, we begin with a trial path, and use many iterations of the Metropolis algorithm to generate new ones. The Metropolis algorithm is a Markov chain Monte Carlo method using importance sampling [1]. This means that in one iteration of this method, a given point on the path with value x has

[1] Where the random points are generated with highest probability in the region of interest.

a probability $W(x, x')$ to be replaced with a new point x', where $W(x, x')$ is called the transition matrix. In the Metropolis algorithm, the transition matrix is given by:

$$W(x,x') = A\Bigg((\theta[S(x_j) - S(x'_j)] + \exp[-\Delta S(x'_j, x_j)]\theta[S(x'_j) - S(x_j)] + \int dx'(1 - \exp[-\Delta S(x'_j, x_j)])\theta[S(x') - S(x_j)]\delta(x'_j - x_j)\Bigg) \tag{2.1}$$

where A is a normalizing constant, $\Delta S(x'_j, x_j) = S(x'_j) - S(x_j)$, and θ is the Heaviside function. Note that from here on we use units where $\hbar = 1$.

This means that for a given lattice site j, a new point x'_j is chosen at random, with uniform probability. If the action of the path is lowered by replacing the value at j with x'_j, then the replacement occurs. Otherwise, it only occurs with probability $\exp(-\Delta S)$ [2].

The new point x'_j is chosen to be in the region $x_j - \Delta < x'_j < x_j + \Delta$, where the value of Δ is chosen in order to optimize the probability that the new x_j is accepted, as discussed in section 3.3.

With this choice of the transition matrix, the condition of detailed balance is satisfied:

$$\frac{W(x,x')}{W(x',x)} = \frac{P(x')}{P(x)} \tag{2.2}$$

Where $P(x)$ is the equilibrium probability density as defined in equation (1.5). Satisfying this condition ensures that after many iterations, the paths we generate follow the required distribution. Once equilibrium is established, any further paths will also be equilibirum paths [2].

2.2 Reaching equilibrium

In our simulations, we begin with the trial path $x_j = 0 \ \forall \ j$. At first, the new paths generated from successive iterations will not be in equilibrium. One way of seeing if the paths are in equilibrium is to look at the evolution of an observable.

For example, consider figure 2.1. The mean square position starts at 0, and grows with each iteration. After approximately 300 iterations, the value is near 0.5 – the theoretical expectation value – and after that there are just statistical fluctuations. In this example, we would wait at least 1000 iterations before making measurements, as it is difficult to tell exactly when equilibrium is reached, and the computational cost of further iterations is low.

It can also be seen in figure 2.1 that the values of $\langle x^2 \rangle$ for paths separated by few iterations are correlated. It is important to take account of this when making measurements. This is discussed in section 3.2.

3 The harmonic oscillator

3.1 Mean square position

The first measurement we made was the mean square position of the harmonic oscillator, as a function of the lattice spacing. This can be compared with the analytical expression from discrete lattice theory [2]:

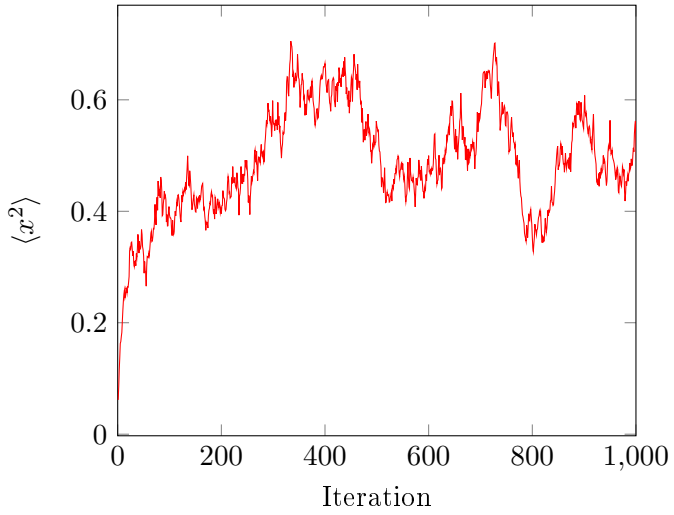

Figure 2.1: The evolution of $\langle x^2 \rangle$ with iterations of the Metropolis algorithm for lattice spacing $a = 0.1$, $\mu^2 = 1$.

$$\langle x^2 \rangle = \frac{1}{2\mu(1 + a^2\mu^2/4)^{1/2}} \left(\frac{1 + R^N}{1 - R^N} \right) \tag{3.1}$$

where $R = 1 + a^2\mu^2 - a\mu(1 + a^2\mu^2/4)^{1/2}$. Figure 3.1 shows the values obtained from simulations at many different lattice spacings.

Motivated by the expansion of the theoretical formula which has a quadratic term as leading order term, we plotted $\langle x^2 \rangle$ as a function of lattice spacing squared. For small values of a^2 the data points approach a straight line, which confirms the leading order being quadratic. We also applied a fit of the form $c_1 + c_2 a^2 + c_3 a^4$ to the data points. The results of this fit were:

$$\begin{aligned} c_1 &= 0.4997 \pm 0.0002 \\ c_2 &= -0.062 \pm 0.002 \\ c_3 &= 0.012 \pm 0.004 \end{aligned}$$

The value for c_1 gives the expectation value for the square position. We can see that this agrees moderately well with the theoretical expectation value, which is $\langle x^2 \rangle = 0.5$, the difference being less than 2 standard deviations. To generate this data, we used equation (3.4) to find the autocorrelation time(see 3.2).

3.2 Autocorrelation

As previously mentioned, a path that is generated from another path stays correlated with this path until there are enough iterations in between them. It is important to be able to estimate how many iterations are required between paths in order for them to be uncorrelated. We did this by measuring the autocorrelation function

$$\Gamma(t) = \frac{\langle (y(0) - \bar{y})(y(t) - \bar{y}) \rangle}{\langle (y(0) - \bar{y})^2 \rangle} \tag{3.2}$$

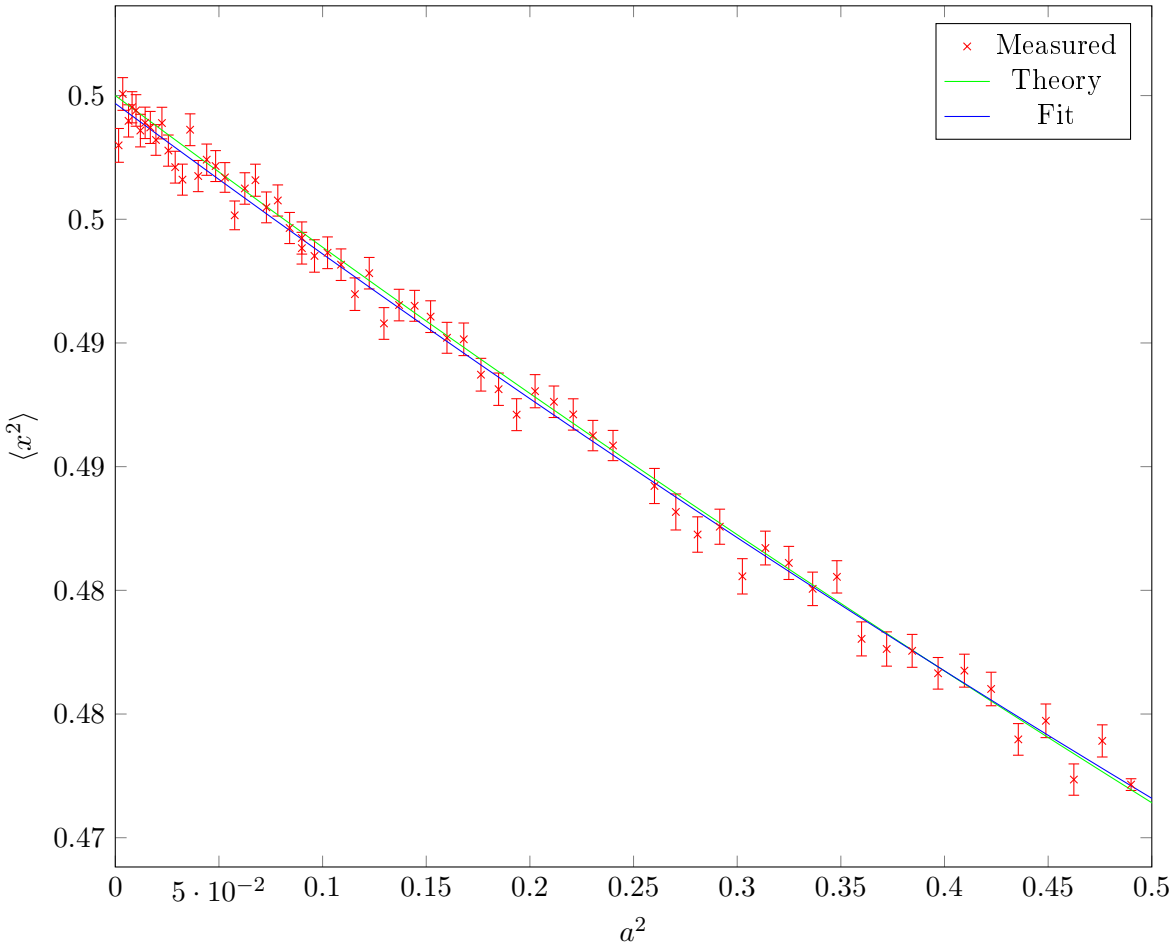

Figure 3.1: $\langle x^2 \rangle$ as a function of lattice spacing squared, with the theoretical curve and a quadratic fit.

where t is Monte Carlo time (number of iterations), y is some observable, and $\bar{y}$ is the mean of the measured values of y. The autocorrelation function should decay exponentially with t [3]:

$$\Gamma(t) = \exp(-t/\tau) \tag{3.3}$$

τ is the autocorrelation time. It gives a measure of the number of iterations needed between measurements. In this section we use $y = x^2$ throughout.

In figure 3.2 we plot the autocorrelation function measured for a lattice spacing of $a = 0.05$ and in figure 3.3 is the logarithm of this autocorrelation function. As can be seen, the expected exponential dependence is observed at low t, but at $t \sim 200$ large statistical fluctuations start to occur. By applying a straight line fit to the plot of $\log(\Gamma)$, the autocorrelation time may be measured.

Figure 3.4 shows the autocorrelation time measured in this manner, as a function of lattice spacing. A log-log plot of this data is displayed in figure 3.5. In this plot, it can be seen that for lattice spacing smaller than about 0.4, the data follows a straight line, indicating that the autocorrelation time is a power law function of the lattice spacing.

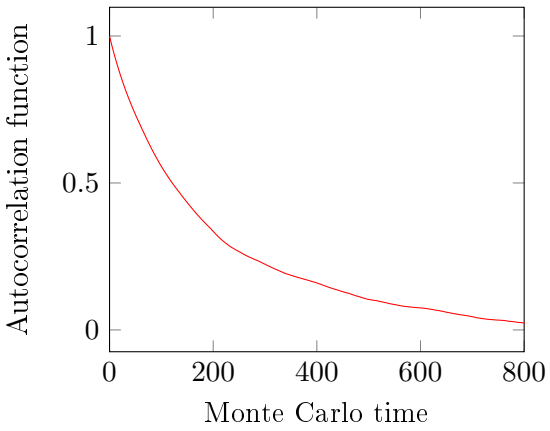

Figure 3.2: The autocorrelation function for $a = 0.05$, $\mu^2 = 1$, $m = 1$.

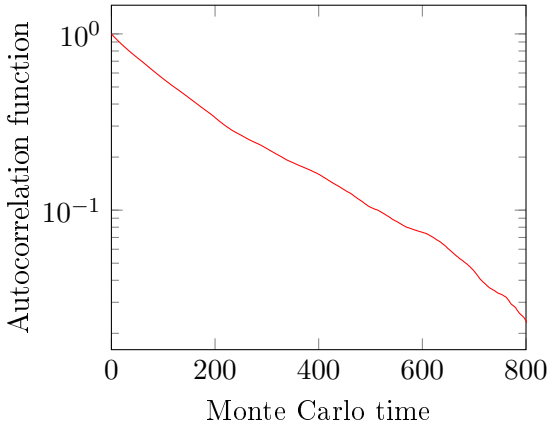

Figure 3.3: Log plot of the autocorrelation function for $a = 0.05$, $\mu^2 = 1$, $m = 1$.

Applying a straight line fit to the data gives $\log(\tau) = -0.49(2) - 1.74(1)\log(a)$. The autocorrelation time in the range $a \in [0.02, 0.4]$ is then given by:

$$\tau = 0.61a^{-1.74} \tag{3.4}$$

For $a \gtrsim 0.4$ this equation no longer holds, and the autocorrelation time stays approximately constant at $\tau = 2$. It is important to note that equation (3.4) only applies for measurements of x^2. For other observables, the autocorrelation time may be different.

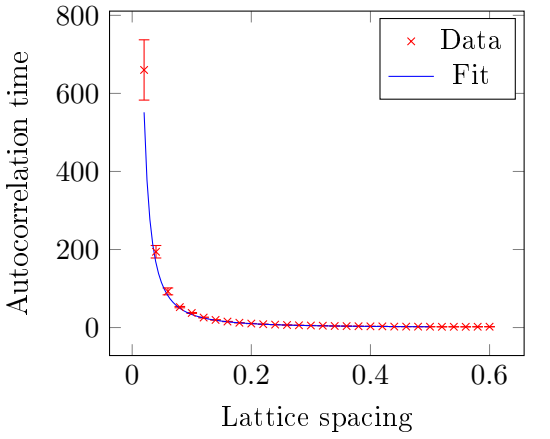

Figure 3.4: The autocorrelation time as a function of lattice spacing for $\mu = 1$, $m = 1$.

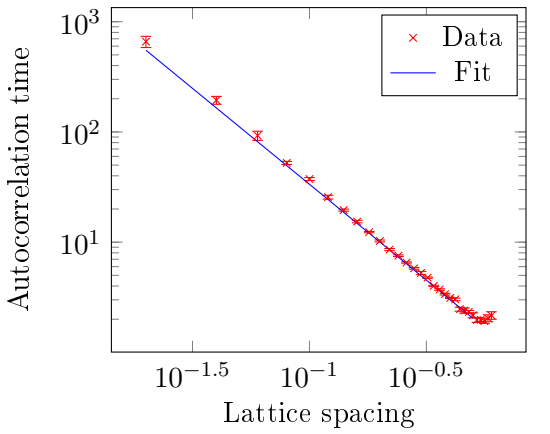

Figure 3.5: log-log plot of the autocorrelationtime as a function of lattice spacing for $\mu = 1$, $m = 1$.

3.3 Optimizing Δ

In the Metropolis algorithm, new values are chosen for the lattice site in the range $x_j - \Delta < x_j' < x_j + \Delta$. In this section we discuss the choice of the parameter Δ.

The value of Δ affects the probability that a new point will be accepted by the Metropolis algorithm, as for large Δ, the change in action is likely to be very large, and hence the probability of acceptance will be small. It also affects the autocorrelation time. For small Δ it will take many iterations for the value of a given lattice site to change significantly, giving a large autocorrelation time. Conversely for large Δ the probability of acceptance is low, leading also to a large autocorrelation time. It is therefore expected that there is some optimal value of Δ for which the autocorrelation time is at a minimum.

In figure 3.6 we plot the measured autocorrelation time and the fraction of accepted trial values of x'_j as a function of Δ, for lattice spacing $a = 0.1$. As expected, there is a minimum in the autocorrelation time, occuring in the range $0.5 < \Delta < 1$, so it is optimal to choose Δ in this range.

Creutz and Freedman [2] choose $\Delta = 2\sqrt{a}$ in their work with the harmonic oscillator, and for $a = 0.1$ this gives $\Delta = 0.63$ which lies within this range. Note that this corresponds to an acceptance probability of approximately 0.5. We find this feature to be quite general, so that a good check that an optimal value of Δ has been chosen is to check that the acceptance probability is 0.5. In all of our work, we use $\Delta = 2\sqrt{a}$.

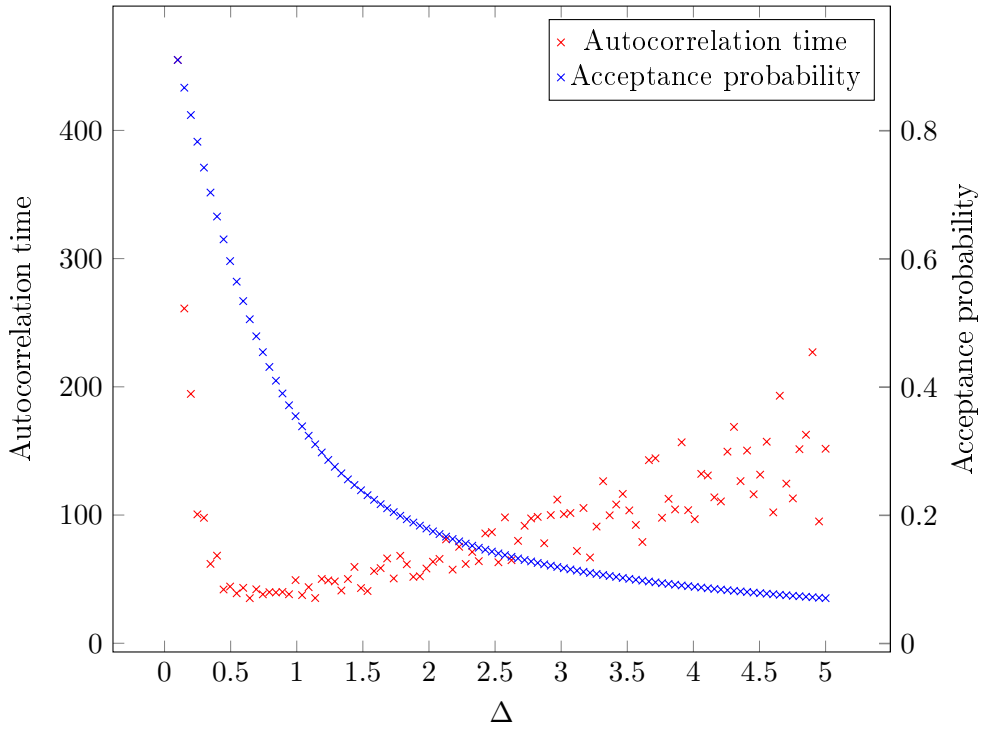

Figure 3.6: The autocorrelation time and the fraction of accepted values of x'_j as a function of Δ for $a = 0.1$, $\mu = 1$, $m = 1$.

3.4 Energy levels

Using our simulations, we computed the energies of the lowest two energy levels of the harmonic oscillator. From the virial theorem, the ground state energy is [4]:

$$E_0 = \mu^2 \langle x^2 \rangle \tag{3.5}$$

For the case $\mu = 1$, in section 3.1 we found the continuum limit $\langle x^2 \rangle = 0.4997 \pm 0.0002$, so we immediately get $E_0 = 0.4997 \pm 0.0002$ for the ground state energy when $\mu^2 = 1$. This compares reasonably well with the theoretical value $E_0 = 0.5$.

To compute the energy of the first excited state, we used a modified version of equation (4.14) from Creutz and Freedman [2]:

$$E_{\text{eff}}(t_L) = -\frac{1}{a} \log \left(\frac{\langle x(0)x(t_L+1) \rangle}{\langle x(0)x(t_L) \rangle} \right) \tag{3.6}$$

We call E_{eff} the effective energy gap. The quantity $\langle x(0)x(t_L+1) \rangle / \langle x(0)x(t_L) \rangle$ is called the correlation function. It is similar to the autocorrelation function, except t_L is the lattice time rather than the Monte Carlo time.

Figure 3.7 shows the effective energy gap for a lattice spacing $a = 0.1$. As can be seen, there is a plateau at $E_{\text{eff}} \approx 1$ for small t, as would be expected. When t becomes too large, the plateau breaks up into statistical fluctuations, these occur because of errors coming from finite machine precision. The reason for this can be seen in figure 3.8. The correlation function rapidly becomes extremely small, and large errors will occur when the ratio of two very small numbers is taken.

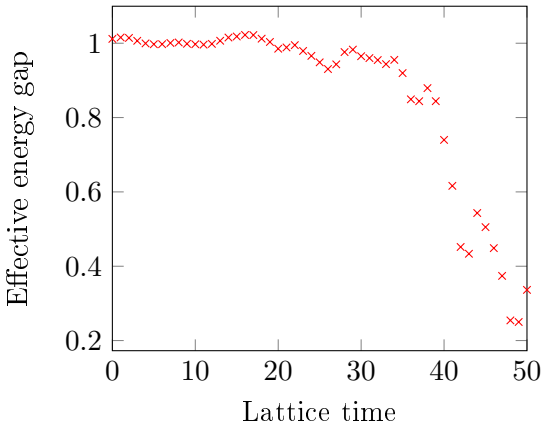

Figure 3.7: The effective energy gap for $a = 0.1$, $\mu^2 = 1$, $m = 1$.

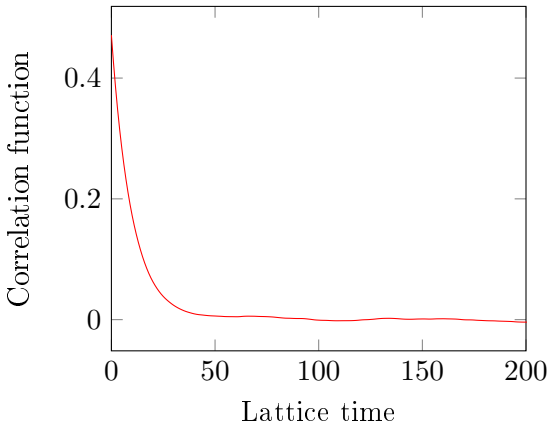

Figure 3.8: The correlation function for $a = 0.1$, $\mu^2 = 1$, $m = 1$.

3.5 Ground state probability density

We measured the ground state probability density following the method of Creutz and Freedman[2] of splitting the x axis into bins, and counting the number of lattice points with values that fall into each bin, for a large number of paths. Dividing this by the total number of points counted gives the ground state probability density. Figure 3.9 shows the measured probability density for $\mu^2 = 1$ and $a = 0.1$. We also plot the theoretical prediction from discrete lattice theory. The measured distribution agrees well with theory.

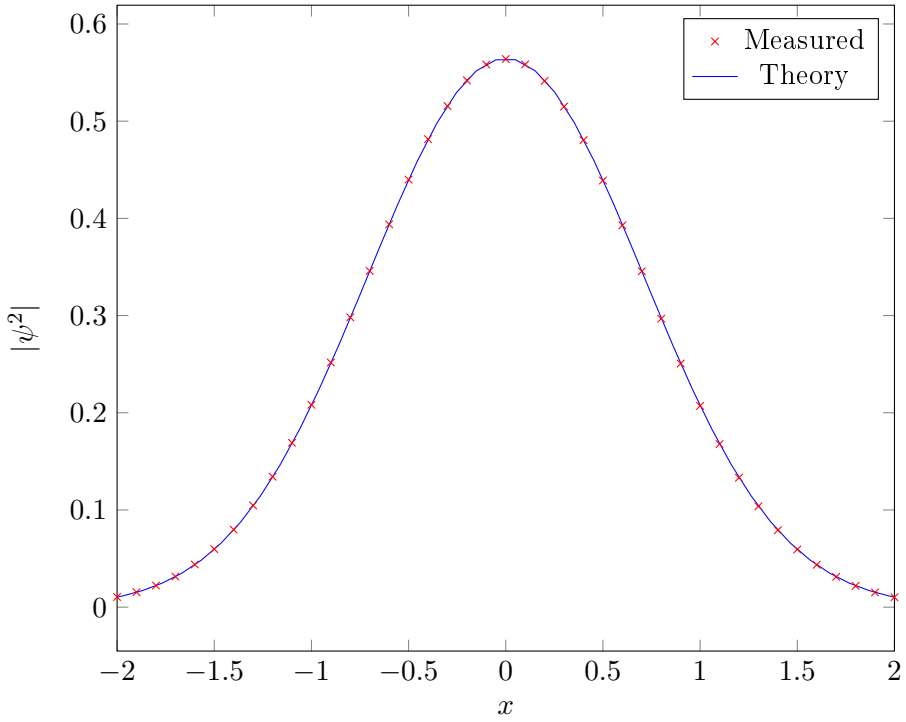

Figure 3.9: The ground state probability density for the harmonic oscillator with $\mu^2 = 1$, $m = 1$.

4 The anharmonic oscillator

4.1 Energy levels

We measured the energy levels of the anharmonic oscillator in the same way as for the harmonic oscillator. For this section we used a slightly modified potential:

$$V(x) = \lambda(x^2 - f^2)^2 \tag{4.1}$$

in order to compare with R. Blankenbecler et al [5]. To compare, we used parameters $m = 0.5$ and $\lambda = 1$ and varied f^2. We made measurements for $a = 0.1$ and $a = 0.05$. Our results are given in table 1.

In figure 4.1 we plot the measured energy levels and the theoretical values [5]. There is good agreement for $f^2 < 1$, but for values of f^2 larger than this the results diverge slightly. This may be due to the finite lattice spacing. The fact that there is much better agreement for $a = 0.05$ than $a = 0.1$ supports this.

4.2 Ground state probability density

In the same manner as described in section 3.5 we computed the ground state probability density for the anharmonic oscillator, using the original action 1.4. The result for $\mu^2 = -4$ and $\lambda = 1$ is plotted in figure 4.2. We found that we needed to measure over a large number of paths, as otherwise the peaks tended to be different heights.

	$a = 0.1$		$a = 0.05$	
f^2	E_0	E_1	E_0	E_1
5	3.99 ± 0.02	4.00 ± 0.02	4.25 ± 0.02	4.30 ± 0.03
4	3.60 ± 0.01	3.60 ± 0.02	3.77 ± 0.02	3.25 ± 0.03
3	3.089 ± 0.010	3.14 ± 0.02	3.21 ± 0.02	3.25 ± 0.02
2	2.223 ± 0.007	2.68 ± 0.03	2.27 ± 0.01	2.74 ± 0.03
1	1.111 ± 0.002	2.68 ± 0.06	1.130 ± 0.004	2.71 ± 0.05
0	1.042 ± 0.001	3.77 ± 0.05	1.0533 ± 0.001	3.81 ± 0.04
-1	2.642 ± 0.001	6.35 ± 0.07	2.669 ± 0.002	6.40 ± 0.05

Table 1: Energy levels of the anharmonic oscillator.

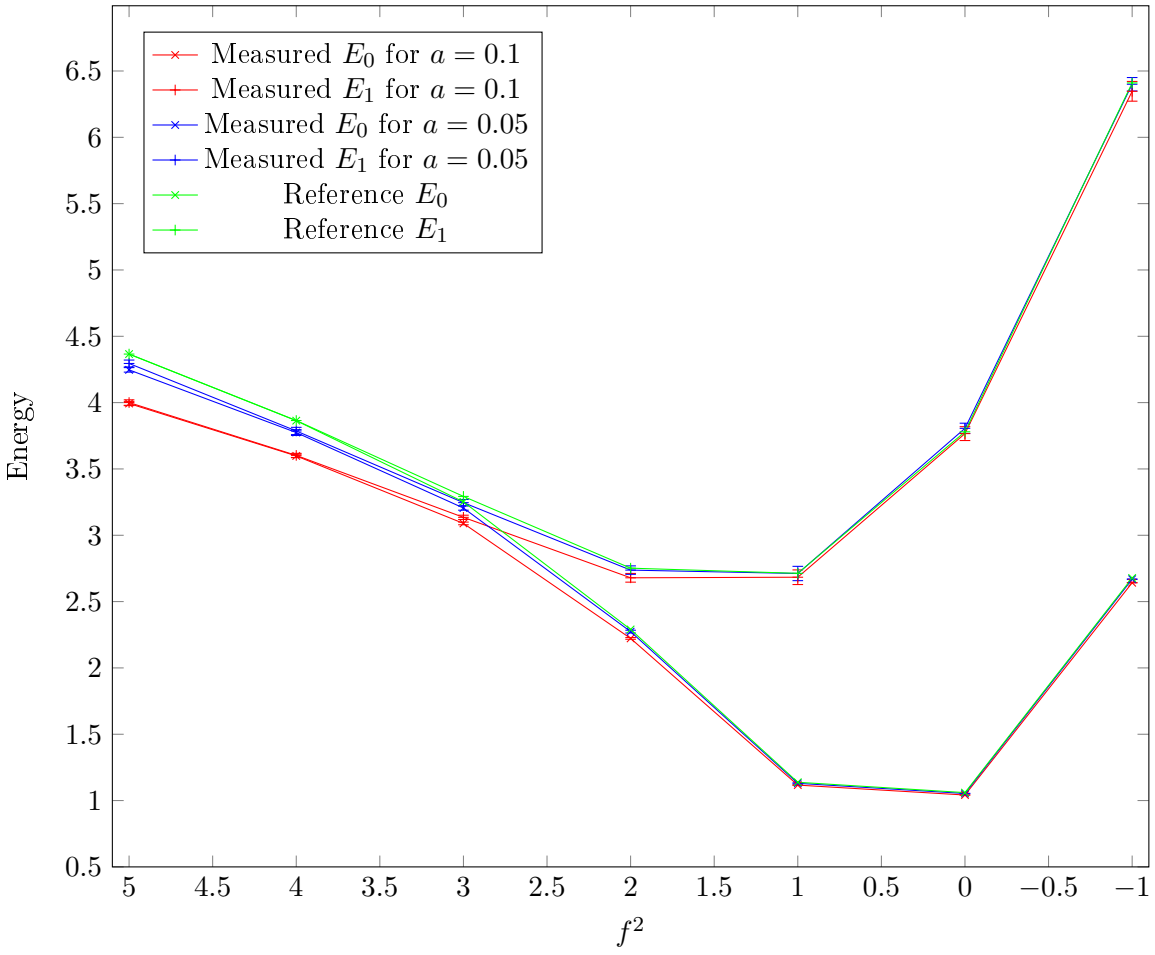

Figure 4.1: The lowest two energy levels of the anharmonic oscillator as a function for f^2 for $m = 0.5$ and $\lambda = 1$.

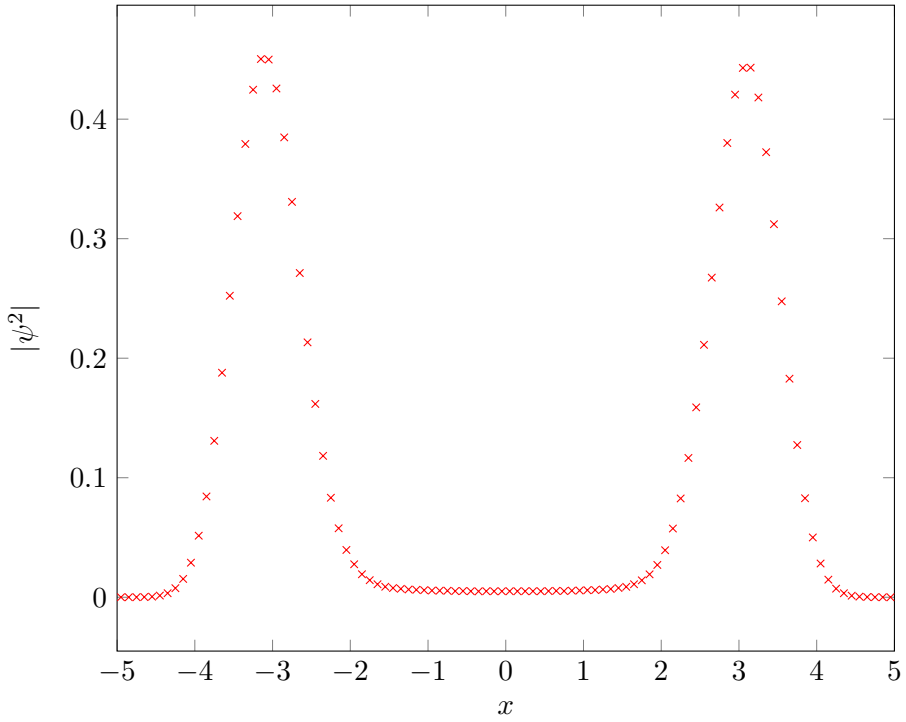

Figure 4.2: The ground state probability density for the anharmonic oscillator with $\mu^2 = -4$ and $\lambda = 0.1$.

5 Conclusions

We have studied quantum mechanical harmonic and anharmonic oscillators using Monte Carlo simulations with the Metropolis method, and used it to calculate several observables. For the harmonic oscillator these agree well with theory. For the energy levels of the anharmonic oscillator, the agreement seems to depend strongly on the lattice spacing used.

This method is unnecessary for the harmonic oscillator, where analytic solutions are available, but it is useful for the study of more complicated systems such as the anharmonic oscillator. In particular, techniques developed here are used in the field lattice quantum chromodynamics. Additionally, it was useful for us to study the harmonic oscillator first in order to check that our understanding and our programs were both correct.

All of the calculations we made were for finite lattice spacing. To obtain a more accurate continuum value, smaller lattice spacings are required. This has the drawback of significantly increasing computation time, as the lattice size must be made larger, and the autocorrelation time increases rapidly with decreasing lattice spacing. For lattice QCD, where both space and time are discretized, supercomputers must be used.

Acknowledgements

We would like to thank Karl Jansen and Krzysztof Cichy, for their patient guidance while we looked for bugs in our code. We would also like to thank Karl for running the DESY Zeuthen summer student program. Christian Wiese provided a working version of the Ranlux random number generator, and both he and Dina Alexandrou made several useful comments and suggestions over the course of our project, for which we are grateful.

References

[1] R. Feynman and A. Hibbs, *Quantum Mechanics and Path Integrals*, Dover (2005)

[2] M. Creutz and B. Freedman, *A Statistical Approach to Quantum Mechanics*, Annals of Physics, **132**, 427-462 (1981).

[3] G.M. Bendia, *Comparison Between the Langevin and the Hybrid Simulation Techniques for a Free Field Theory*, J. Phys., **22**, 5065 (1989).

[4] J. Binney and D. Skinner, *The Physics of Quantum Mechanics*, Oxford University Press (2013).

[5] R. Blankenbecler, T. DeGrand and R. L. Sugar, *Moment method for eigenvalues and expectation values.* Phys. Rev., **21**, 1055 (1980).

A The kernel for the harmonic oscillator

We wish to compute the kernel to go from x_a to x_b for a harmonic oscillator. We do this by looking at the classical path and adding fluctuations around it:

$$x = \bar{x} + y \tag{A.1}$$

where $\bar{x}$ is the classical path and y is the fluctuation. The Lagrangian for the harmonic oscillator then becomes

$$L = \frac{m}{2}\dot{\bar{x}}^2 - \frac{m\omega^2}{2}\bar{x}^2 + \frac{m}{2}\dot{y}^2 - \frac{m\omega^2}{2}y^2 + m\dot{\bar{x}} - m\omega^2\bar{x}y \tag{A.2}$$

The action for the harmonic oscillator on a path from the point (x_a, t_a) to (x_b, t_b) is then

$$S = \int_{t_a}^{t_b} \left(\frac{m}{2}\dot{\bar{x}} - \frac{m\omega^2}{2}\bar{x}^2 + \frac{m}{2}\dot{y}^2 - \frac{m\omega^2}{2}y^2 + m\dot{\bar{x}} - m\omega^2\bar{x}y \right) dt \tag{A.3}$$

where the last two terms, which are linear in y or $\dot{y}$ disappear by definition of the classical path as the path the extremises the action. The classical action can then be factored out of the equation for the kernel

$$K(b,a) = \mathrm{e}^{(\mathrm{i}/\hbar)S_{\mathrm{cl}}[b,a]} \int_0^0 \left(\exp\left\{ \frac{i}{\hbar} \int_{t_a}^{t_b} \left[\frac{m}{2}\dot{y}^2 - \frac{m\omega^2}{2}y^2 \right] \right\} \right) \mathcal{D}y(t) \tag{A.4}$$

Since $y(t_a) = y(t_b) = 0$, the integral over the fluctuations can be a function only of the start and end times t_a and t_b. Further, since the Lagrangian is not an explicit function of time, the action remains the same under a change of integration variable to $t' = t - t_a$. The integral for the action then runs from $t' = 0$ to $t' = T = t_b - t_a$, and so the kernel takes the form

$$K = F(T)\mathrm{e}^{(\mathrm{i}/\hbar)S_{\mathrm{cl}}[b,a]} \tag{A.5}$$

A.1 The classical action

From the Euler-Lagrange equation for the simple harmonic oscillator,

$$\ddot{\bar{x}} = -\omega^2\bar{x} \tag{A.6}$$

the classical path is

$$\bar{x} = A\cos(\omega t') + B\sin(\omega t') \tag{A.7}$$

where A and B are constants which depend on initial conditions. Substituting this path into the integral for the classical action gives

$$\begin{aligned} S_{\mathrm{cl}} &= \frac{m\omega^2}{2}\int_0^T [(A\sin(\omega t') - B\cos(\omega t'))^2 - (A\cos(\omega t') + B\sin(\omega t'))^2]dt' && \text{(A.8)} \\ &= \frac{m\omega^2}{2}\int_0^T [A^2\sin^2(\omega t') + B^2\cos^2(\omega t') - 2AB\sin(\omega t')\cos(\omega t') && \text{(A.9)} \\ &\quad -A^2\cos^2(\omega t') - B^2\sin^2(\omega t') - 2AB\sin(\omega t')\cos(\omega t')]dt' && \text{(A.10)} \\ &= \frac{m\omega^2}{2}\int_0^T [(B^2 - A^2)\cos(2\omega t') - 2AB\sin(2\omega t')]dt' && \text{(A.11)} \end{aligned}$$

Next, we use the initial conditions $\bar{x}(t_a) = x_a$ and $\bar{x}(t_b) = x_b$ to determine A and B.

$$\text{at } t' = 0: \qquad \bar{x} = x_a \qquad \Rightarrow \qquad A = x_a \tag{A.12}$$

$$\text{at } t' = T: \qquad \bar{x} = x_b \qquad \Rightarrow \qquad B = \frac{x_b - x_a \cos(\omega T)}{\sin(\omega T)} \tag{A.13}$$

Substituting these into the equation for the action gives the result:

$$S_{\text{cl}} = \frac{m\omega}{2\sin(\omega T)}[(x_a^2 + x_b^2)\sin(\omega T) - 2x_a x_b] \tag{A.14}$$

A.2 The path integral over the fluctuations

We wish to evaluate

$$F(T) = \int_0^0 \left(\exp\left\{ \frac{i}{\hbar} \int_{t_a}^{t_b} \left[\frac{m}{2}\dot{y}^2 - \frac{m\omega^2}{2} y^2 \right] \right\} \right) \mathcal{D}y(t) \tag{A.15}$$

$$= \lim_{\epsilon \to 0} \left(\frac{m}{2\pi \mathrm{i}\hbar t} \right)^{N/2} \times \int \cdots \int \exp\left\{ \frac{\mathrm{i}m}{2\hbar\epsilon} \sum_{p=1}^{N-1} [(y_n - y_{n-1})^2 - \omega^2 \epsilon^2 y_n^2] \right\} dy_1 \cdots dy_{N-1} \tag{A.16}$$

We must have $y_0 = y_N = 0$, so we may write the y_n as a sine series

$$y_n = \sum_{p=1}^{N-1} \tilde{y}_p \sin\left(\frac{\pi p n}{N} \right) \tag{A.17}$$

Using the results

$$\sum_{n=1}^{N-1} y_n^2 = \sum_{n,p,q} \tilde{y}_p \tilde{y}_q \sin\left(\frac{\pi p n}{N} \right) \sin\left(\frac{\pi q n}{N} \right) \tag{A.18}$$

$$= \frac{N}{2} \sum_p \tilde{y}_p^2 \tag{A.19}$$

and

$$\sum_{n=1}^{N-1} (y_n - y_{n-1})^2 = \sum_{n,p,q} \left(\tilde{y}_p \sin\left(\frac{\pi p n}{N} \right) - \tilde{y}_p \sin\left(\frac{\pi p (n-1)}{N} \right) \right) \times \left(\tilde{y}_q \sin\left(\frac{\pi q n}{N} \right) - \tilde{y}_q \sin\left(\frac{\pi q (n-1)}{N} \right) \right) \tag{A.20}$$

$$\to 2N \sum_p \sin^2\left(\frac{\pi p}{2N} \right) \tilde{y}_p \tag{A.21}$$

the argument of the exponential is diagonalised. Changing the integration variables to the $\tilde{y_p}$, the Jacobian is independent of $\tilde{y_p}$ (since the transformation is linear) and ω. It therefore simply becomes a constant factor at the front of the integral. Hence, we have

$$F(T) \propto \prod_{p=1}^{N-1} \int_\infty^\infty \exp\left\{ \frac{imN}{2\hbar\epsilon} \left[2\sin^2\left(\frac{\pi p}{2N} \right) - \frac{\omega^2\epsilon^2}{2} \right] \tilde{y}_p \right\} d\tilde{y}_p \tag{A.22}$$

$$\propto \prod_{p=1}^{N-1} \left(4\sin^2\left(\frac{\pi p}{2N} \right) - \omega^2\epsilon^2 \right)^{-1/2} \tag{A.23}$$

For large N, this becomes

$$F(T) \propto \prod_{p=1}^{N-1} \left(\left(\frac{\pi p}{2N} \right)^2 - \omega^2 \epsilon^2 \right)^{-1/2} \tag{A.24}$$

$$= C \prod_{p=1}^{N-1} \left(1 - \frac{\omega^2 \epsilon^2 N^2}{\pi^2 p^2} \right)^{-1/2} \tag{A.25}$$

The product may be evaluated using Stirling's formula, giving the result

$$F(T) = C \left(\frac{\omega T}{\sin(\omega T)} \right)^{1/2} \tag{A.26}$$

with $N\epsilon = T$. To determine the constant factor, we take the limit $\omega \to 0$ and compare our result with the known result for a free particle [1], giving $C = (m/2\pi \mathrm{i}\hbar T)^{1/2}$. The kernel for the harmonic oscillator is then

$$K = \left(\frac{m\omega}{2\pi \mathrm{i}\hbar \sin(\omega T)} \right)^{1/2} \exp\left(\frac{im\omega}{2\hbar \sin(\omega T)} [(x_a^2 + x_b^2)\sin(\omega T) - 2x_a x_b] \right) \tag{A.27}$$

B Energy gap

Here we derive equation (3.6). Consider

$$\begin{aligned} \langle x(0)x(t) \rangle &= \langle 0|x(0)x(t)|0\rangle \\ &= \sum_{n=0}^{\infty} \langle 0|x(0)|n\rangle\langle n|x(t)|0\rangle \\ &= \sum_{n=0}^{\infty} c_n e^{-(E_n - E_0)t} \end{aligned}$$

where $c_n = |\langle 0|x(0)|n\rangle|^2$ and we have used the result $x(t) = e^{-Ht}x(0)e^{Ht}$ (recall that we are working with imaginary time). Note that

$$\begin{aligned} \langle x(0)\rangle\langle x(t)\rangle &= \langle 0|x(0)|0\rangle\langle 0|x(t)|0\rangle \\ &= \langle 0|x(0)|0\rangle\langle 0|x(0)|0\rangle \\ &= c_0 \end{aligned}$$

Due to the symmetry of the potential, $\langle x(0)\rangle = 0$ (within error), so the sum may be rewritten:

$$\langle x(0)x(t) = \rangle \sum_{n=1}^{\infty} \langle 0|x(0)|n\rangle\langle n|x(t)|0\rangle \tag{B.1}$$

For large t, the leading term will dominate, giving $\langle x(0)x(t)\rangle = c_1 e^{-(E_1 - E_0)t}$. Hence, for large t

$$\frac{\langle x(0)x(t+1)\rangle}{\langle x(0)x(t)\rangle} = e^{-(E_1 - E_0)t} \tag{B.2}$$

Giving equation (3.6).

C Bootstrap error analysis

For some of the error analysis in our project, we used a bootstrap with blocking method. In this method, given a sample of N random data points $\{X_i\}$, the data is split into blocks, so for example, with a block size of 2, X_1 and X_2 form one block, X_3 and X_4 form the next, and so on. Next, a set of B bootstrap samples are taken, by randomly selecting blocks with replacement, such that each bootstrap sample contains N data points. For each of the samples, we compute the mean value, so we have a set of B bootstrap means $\{\bar{X}_i\}$. The mean and the standard deviation of these give the bootstrap estimate of the mean of the underlying distribution and its standard error. Calculating errors in this manner is useful for reducing the effect on any residual correlations.